

A Review on the Utilization of Waste Material for Autoclaved Aerated Concrete Production[†]

R. A. Rahman¹, A. Fazlizan^{1,*}, N. Asim¹ and A. Thongtha²

¹Solar Energy Research Institute (SERI), Universiti Kebangsaan Malaysia, Bangi, Selangor, 43600, Malaysia

²Department of Physics, Faculty of Science, Naresuan University, Phitsanulok, 65000, Thailand

*Corresponding Author: A. Fazlizan. Email: a.fazlizan@ukm.edu.my

Received: 01 August 2020; Accepted: 13 October 2020

Abstract: Autoclaved aerated concrete (AAC) has become more attractive due to its excellent and environmental-friendly properties in building construction. AAC is relatively lightweight, possesses lower thermal conductivity, higher heat resistance, lower shrinkage, and faster construction than normal concrete. AAC is a combination of silica sand, cement, gypsum, lime, water, and an expansion agent. To improve its physical and mechanical properties and reduce its production cost, tremendous innovations where waste materials were utilized as partial replacement of AAC materials were done. This paper is intended to present the literature on the utilization of waste materials as a means of a partial replacement in AAC materials to enhance its physical and mechanical properties and thermal performance. The physical properties such as microstructure and mechanical properties such as density, compressive strength, water absorption are presented to classify the investigation that has been done in such innovations. Apart from that, the discussion on innovations to improve its thermal performance was also presented. Based on the review, an increase of AAC application causes much waste at construction sites and recycling concrete waste powder into wall concrete; particularly, an AAC was not frequently practiced in construction.

Keywords: Autoclaved aerated concrete; microstructure; waste material; compressive strength

1 Introduction

Construction works to build structures such as commercial buildings, high-rise buildings, building offices, and residential are rapidly growing significantly in developing countries, including Malaysia. Due to its excellent mechanical features, low cost and availability, concrete is a primary building material for most residential buildings. However, large-scale construction requires large building structures and foundation, resulting in the consumption of even more time and expenses.

[†] This paper is an extended and revised article presented at the International Conference on Sustainable Energy and Green Technology 2019 (SEGT 2019) 11–14 December 2019 in Bangkok, Thailand.



This work is licensed under a Creative Commons Attribution 4.0 International License, which permits unrestricted use, distribution, and reproduction in any medium, provided the original work is properly cited.

The Monsoon region's environmental condition, which includes the countries of Southeast Asia, is warm and humid, causing the heat and moisture accumulation in the construction wall, which then affects the building materials' thermal performance and the energy consumption of the building [1,2]. As a consequence, ventilating ventilators and/or air-conditioners reduces heat and provides the building occupants with a calm conducive environment [3–5]. Meanwhile, both economic and energy crises have stimulated energy conservation awareness, resulting in a drastic increment of construction material studies that integrates energy conservation [6].

One of the approaches to maximize energy efficiency in buildings is to use lightweight construction materials with lower thermal conductivity and higher heat resistance. One of the famous building materials that have these is autoclaved aerated concrete (AAC). AAC is chosen due to its environmentally friendly characteristics and has excellent thermal insulation. Generally, AAC is relatively lightweight and possesses better heat resistance, low thermal conductivity, lower shrinkage, and faster construction than standard concrete [7–10]. Because of its ability to minimize building energy consumption by about 50 percent without applying thermal insulation layers to the building wall, AAC can be deemed a green or environmental-friendly building material [11].

In preventing heat transfer into the building interior, many kinds of literature were reported using an insulator as a building material. Khedari et al. [12] reported that an internal concrete structure consisting of durian fibers and coconut then mixed with sand and cement in different proportions could exhibit lightweight characteristics. It shows that additive fiber blocks' low density and thermal conductivity could help prevent heat transfer to build-in. Nevertheless, it only could be recommended for non-load-bearing units of concrete masonry because of their low compressive strength [12]. John et al. [13] performed an evaluation of degradation on a composite wall panel which made of clinker-free, low alkaline, activated coconut fiber-fortified slag cement. Although the decomposition and leaching of lignin in the fibres could not prevent the low alkaline cement from lignin's leaching, it negligible the effect on the wall's performance.

In addition, cement and many other additives, such as ash, zeolite, or polystyrene foam, were used in different non-autoclaved and autoclaved lightweight concrete experiments to explain its structures and engineering properties [13–15]. For example, the effect of polymer cement modifiers was investigated on the mechanical and physical properties of mortar using waste concrete fine aggregate, and it was found that by adding higher polyacrylic ester (PAE) modifier material, mortar porosity could increase [16]. Hot water resistance and higher compressive strength but lower flexural strength could be enhanced by such a polymeric modifier [17].

Many studies have shown that either fine sands or cement replacement could increase its strength, reduce density and thermal conductivity, and some other characteristics [18]. In addition to improving its properties, AAC research also requires partial replacement of waste materials by materials that lead to lower production costs, thus reducing the cost of AAC construction [18–23].

2 AAC Manufacturing Process

Aerated concrete can be classified as autoclaved aerated concrete (AAC) and non-autoclaved aerated concrete (NAAC) based on the process of pore-formation, the type of binder, and the method of curing [24]. The AAC properties such as drying shrinkage compressive strength, water absorption, and density directly vary on the curing process and duration. Fig. 1 below shows the process difference in preparing aerated concrete between the NAAC (also known as foamed concrete) and AAC.

AAC that has been used in current masonry units had an entrapped air voids product of combining silica sand, cement, gypsum, lime, water, and aluminum powder as an expansion agent [25]. In the mixture, the aluminum powder that serves as an expansion agent will react with the silica, resulting in the formation of millions of microscopic hydrogen bubbles [26]. The hydrogen then subsequently evaporates and

leaving a highly closed-cell aerated concrete. The partially dried aerated concrete is cut into blocks or panels steamed and pressure-cured in an autoclave [24].

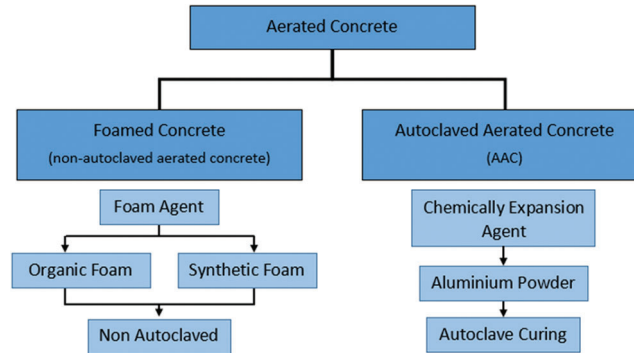


Figure 1: Process flow of the preparation of aerated concrete between the foamed concrete (NAAC) and AAC

Also, the production methods for autoclaved aerated concrete consist of two types, chemical, and mechanical processes. The chemical response of aluminum paste makes it a porous shape having mild weight and more luxurious insulation houses making one-of-a-kind from different mild weight concrete [27]. Many metallic compounds will be used in the chemical process to react and produce enormous quantities of air bubbles in the textured concrete. In contrast, a vast foaming agent is usually used in mechanical processes [27]. In general, AAC can be prepared under temperature and pressure conditions greater than 180°C and 12 bar, respectively, in a high-pressure autoclave [28].

3 Chemical Composition in AAC

XRD analysis could determine the main mineralogical materials in AAC, which normally appears are tobermorite and fine-crystalline C-S-H [29]. In preparing the materials replacement or addition of additives in AAC, tobermorite stabilization or C/S ratio should be taken for determining the crystalline phases of formation and micro-morphology. Tobermorite can be stabilized with a C/S ratio of 0.8 to 1.0 and a temperature of up to 150°C with the aid of an autoclave process [30]. At C/S ratio greater than 1, C-S-H transform to a needle-like tobermorite due to shorter chains of silica and dimers; hence C-S-H repositions more efficiently [31]. However, tobermorite's increase could reduce the C/S ratio from 1.69 to 0.9 [32]. At a superficial level of C/S ratio, which is less than 0.8, the C-S-H, which is normally formed like a grass-type structure. Normally, the C/S ratio for the formation of tobermorite is in the range from 0.8 to 1 [33].

Tobermorite is normally found in the layer of tetrahedral silicate and octahedral calcium [34]. A two-step process can form the C-S-H system with the hydrothermal reaction between SiO_2 and Ca(OH)_2 as a slurry phase. In the first step, the SiO_2 surface produces C-S-H gel and then reacts with Ca(OH)_2 to form a standard crystalline. The curing of crystalline products will be considered in the second stage. During the autoclave curing process, where high pressure (10–12 bar) and temperature (180–190°C) occurs, tobermorite can be formed [34].

Autoclaving is necessary to form crystalline phases, but tobermorite formation would require excessive prolongation in the autoclave [29]. Mostafa [20] highlighted that the tobermorite phase strength did not improve after 2 h of autoclaving. Simultaneously, by increasing the time needed for autoclaving, which is from 8 h to 18 h, the mechanical and microstructural characteristics remained stable after 8 h. Autoclaving prolongation would not affect the tobermorite phase [28], suggesting that tobermorite

formation was inhibited after 8 h of autoclaving. Relevant autoclave or steam pressure used can be due to this difference in the early preventing autoclaving time. Previous research shows that the existence of Al^{3+} speed up the tobermorite crystallization rate [35–37], and leads to an increase of the c unit-cell parameter, while the substitution of $(SO_4)^{2-}$ give no effect [38]. The addition of Al^{3+} also lowers the autoclaving temperature and reduces the autoclaving time for tobermorite formation [20,36].

Bergold [39] presents the quantitative phase analysis of hydrating cement pastes, showing that the Rietveld refinement of an *in-situ* XRD pattern after 65 h of hydration at 23°C and water to solid ratio of 0.5. The phases determined are alite, portlandite and C-S-H. In contrast, other XRD analysis shows that tobermorite and crystalline C-S-H are the main components in AAC [20,23,26,28,35,40,41]. Secondary phases such as xonotlite, jennite, and other calcium silicate hydrates regularly appear depending on autoclaving temperature and time and C/S ratio [28,42,43].

4 Material Replacement in AAC Production

The development of AAC is divided into two types: Lime-based or cement-based, depending on the dissimilar materials applied, such as sand and fly ash, based on various silica materials or various calcareous materials used [29]. Aluminum powder is a very popular air-entraining agent that could be used to incorporate a trapped void device. In preparation for AAC, fly ash, silica fume, and slag have been increasingly used as supplementary cementitious material. The addition of silica and coal bottom ash in AAC production could increase the density. Apart from that, the excessive addition of more than 30 percent of coal bottom ash may weaken the strength of AAC and may also reduce the amount of absorbent voids due to the decrease in hydrogen gas. However, ash and silica fume variations significantly affect AAC's thermal conductivity [19,44].

Previous researches shown in Tab. 1 are the innovations that have been done by replacing its based materials using waste materials (industrial by-products). These innovations are either to improve AAC characteristics, properties, and performance or the manufacturing cost while maintaining its properties at the acceptable ranges. Besides waste materials, additions or replacement, additives such as fibers, micro-particles, hydrophonic agents and superplastizer are also being applied in AAC preparation [45–48]. These additives also could enhance the properties of AAC, such as an addition of amorphous SiO_2 increased the compressive and flexural strength.

Table 1: Past and present innovations of materials' replacement using industrial by-products to improve AAC properties

Ref.	Materials	Replacement method	Enhancement/Improvement
[26]	S/C/L/Natural Zeolite (NZ)	NZ to replace a portion of sand (optimum at 50%)	Decreases the unit weight of aerated concrete specimens hence decrease density
[25]	S/C/L/Sugar Sediment waste (SSW)	SSW to replace a portion of sand and lime (optimum at 30% of sand and 7.5% of lime)	Higher compressive strength, better thermal resistance, and finer crystalline morphology
[20]	S/C/L/Air-cooled Slag (AS)	AS to replace lime and sand (optimum at 50% low-lime mixes and 30% for high-lime mix)	Improve the strength of compression and shorten the curing times
[44]	FA/C/L/G/Incineration Bottom Ash (IBA)	IBA to replace aluminium powder as an aerating agent and a portion of silica/fly ash	IBA-AAC has higher compressive strength compared to normal AAC at a given density & aluminium dosage
[28,33]	S/C/L/Rice Husk Ash (RHA)	RHA and aluminium containing waste as a partial aggregate and expansive agent replacement	Delicate particle size has a positive effect on the CSH to tobermorite conversion
[49]	C/L/G/Coal Gangue (CG)/Iron Ore Tailings (IOT)	Optimum composition: 20% CGC, 40% (IOT), 25% lime, 10% cement, 5%, 0.06% Al powder	Completely replace sand to achieve bulk density and compressive strength of 609 kg/m ³ and 3.68 MPa, respectively
[50]	C/Pulverized Fuel Ash (PFA)/ Palm Oil Fuel Ash (POFA)	PFA and POFA to completely replace cement	Control heat of hydration

Table 1 (continued).

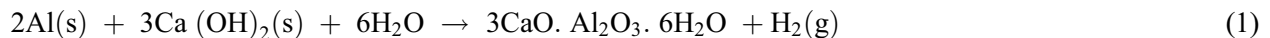
Ref.	Materials	Replacement method	Enhancement/Improvement
[10]	S/C/Palm Oil Fuel Ash (POFA)	POFA to partially replace cement at 20%	Finer particle sizes and pozzolanic reaction favour for strength development
[51]	C/L/G/Self-ignition Coal Gangue (SCG)	Optimal mix proportion is SGC: lime: cement: gypsum = 54: 23: 20: 3 with 1.3% aluminum powder	The products consisted of CSH gel and tobermorite phase.
[23]	S/C/G/Copper Tailing (CT)/ Blast Furnace Slag (BFS)	Mixture composition SCT: BFS: Sand: Cement: Gypsum = 30:35:20: 10:5	The compressive strength was 4.0 MPa, and the dry density was 610.2 kg/m ³
[19]	S/C/L/Coal Bottom Ash (CBA)	CBA to replace sand. Optimum replacement of CBA is 50%	Decreased the thermal conductivity values up to 39% and increased strengths up to 16% higher than reference AAC
[52]	S/C/L/G/Iron Tailing (IT)	IT to substitute sand at 40–60%	The bulk density can be between 490–525 kg/m ³ , compressive and specific strength >2.5 MPa and >4700 N m/kg, respectively
[53]	S/C/L/Perlite Waste (PW)	PW to replace the sand	PW at 10% reduced the thermal conductivity about 15% without significant reduction of compressive strength
[54]	S/C/L/G/Waste Glass (WG)	Various types of WG are used to replace the sand	AAC with cathode ray tube glass has similar characteristics to the reference sample
[55]	C/L/ Silica Fume (SF)/ Fly Ash	5% SF addition	SF can be used as a useful additive to the fly ash/cement-based AAC systems

Note: C = Cement, L = Lime, S = Sand, G = Gypsum, WG = Waste Glass, PW = Perlite Waste

5 Physical Properties

5.1 Density

AAC physical properties reflect its microstructure and density. Most of AAC properties such as drying shrinkage, compressive strength, and thermal conductivity, are closely linked to its density [33]. As an expansion agent, the aluminium powder reacts with calcium hydroxide and water to form hydrogen, which slightly adjusts AAC density, as represents in chemical Eq. (1). The hydrogen gas foams and doubles the raw mix volume, gas bubbles are formed and then evaporate, leaving air voids up to 3 mm in diameter [56,57].



In other words, the material density is inversely proportional to the percentage of air bubbles produced during the expansion process [58]. Other physical characteristics of AAC, such as compressive strength, thermal properties, and drying shrinkage, depending on the AAC density itself. According to ACI Committee Guide 213 for Structural Lightweight Aggregate Concrete, lightweight concrete can be graded according to its unit weight or density, typically ranging from 320 kg/m³ to 1920 kg/m³ [59]. AAC is known as lightweight concrete, where its density values typically range from 300 to 1800 kg/m³ [24]. Further classification of lightweight concrete is classified into three density ranges, i.e., low-density concrete (0.7–2.0 MPa), medium-density concrete (7–14 MPa) and structural concrete (17–63 MPa) with densities ranging from 300–800 kg/m³, 800–1350 kg/m³, and 1350–1920 kg/m³ respectively [56]. Low-density lightweight concrete in construction has a range of advantages due to its low density, low thermal conductivity, low shrinkage, high heat resistance, reduced dead load, lower shipping costs, and higher construction rates [56,60].

5.2 Shrinkage

Drying shrinkage of concrete is defined as contracting the hardened mixture due to the loss of capillary water, leading to increased tensile stress, which may cause crack formation [61]. Due to its high total porosity and the pores' particular surface, drying shrinkage is important in aerated concrete [62]. Lam et al. [63]

suggested that drying shrinkage of AAC is a function of the specific surface area of fine pores of radii 2–20 nm. Additionally, an increase of crystalline content in the substance will also reduce the substance [52]. Drying shrinkage also depends on the quantity of silicate calcium hydrate. In other words, due to the high tobermorite formation, the addition of alumina materials such as high-grade sandblast furnace, bauxite, and high alumina cement will reduce the dry shrinkage by about 30%–100% [25].

5.3 Water Absorption

AAC is known to have high water absorption due to its high porosity and an expansive drainage channel [64]. The amount of water absorption has two parts, i.e., in the capillary hole (pore diameter $< 1 \mu\text{m}$) and in large ventilation port. Typically, there are two categories of pores, namely open pores, which relate to each other and the outside, and blind pores that are not connected. Driven by capillary force, the open pores have a water absorption effect [65]. Soluble salt in the liquid water absorbed into the porous materials may have a damaging impact on steel reinforcement [66]. Besides, the building materials' thermal performance is also affected by liquid water, making the thermal analysis predict the building's energy consumption affected [67].

6 Mechanical Properties

6.1 Compressive Strength

The compressive strength is a measurement of the stress of resistance given by the pores' wall, depends on the pore structure and the binder [27]. In such a way, the pore structure's influence on the compressive strength is primarily more significant than that of the binder's maturity, which is construed by the fact that the average porosity impact to the compressive strength is twice that of the latter [68]. In addition, the reduction in density could decrease its compressive strength and increase its porosity [22,23,28,29,33,44,45,53,64], as shown in Fig. 2. Also, despite similar porosity, small-size pores' increment leads to higher compressive strength [69]. In other words, to achieve both high porosity and elevated strength, the refinement of pore size distribution provides access.

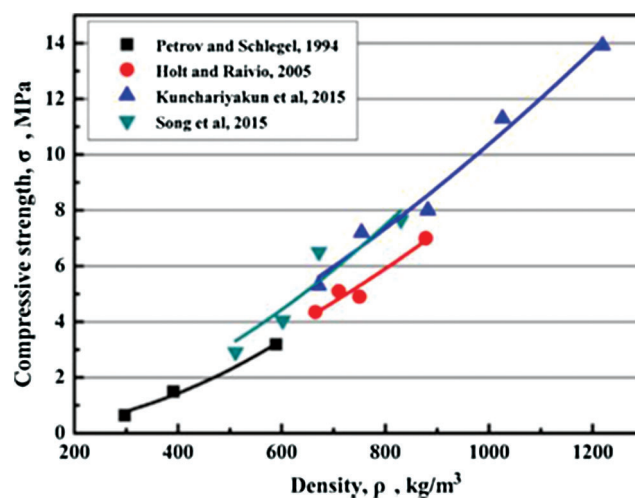


Figure 2: The relationship between compressive strength and density [24]

Generally, the compressive strength increases linearly with density [70]. As high temperature and pressure resulted in a stable form of tobermorite, the Autoclaving process significantly increases the compressive strength. Tobermorite, since it is an important constituent of AAC, is one of the most industrially important calcium silicate hydrates. AAC's mechanical properties are influenced by the

quantity and quality of tobermorite provided by this process [71]. Depending on the autoclaving pressure and length, the final strength is reached, while the compressive strength decreases by decreasing density and increasing porosity, as shown in Fig. 2 below [29].

Jityachaipum in aerated concentrated studies has been conducted by substituting the Portland cement material with fly ash and natural zeolite to improve its strength. Lightweight concrete with comparatively high compressive strengths of 3.65 and 4.51 N/mm², respectively, resulted in 10% by weight [72]. The sand replacement has enhanced its properties in terms of its physical strength, microstructure, and thermal conductivity in aerated concrete itself. Wang et al. [21] improved the microstructure of AAC using recycled clayish crushed stone for aerated concrete production. The hydration products were shown to be poorly crystalline C-S-H, tobermorite and hydrogarnet. Using lead-zinc tailings, Li, Chen, and Long manufactured aerated concrete, which clarified the effects of casting temperature, water-binder ratio, and aluminium powder content on gas-forming actions. Those on the aerated concrete of lead-zinc tailing material, cement content, and conditioning agents [73].

Meanwhile, Mostafa [20] performed a study to increase the compressive strength of lime and sand replacement by up to 50 percent by air-cooled slag of autoclaved aerated concrete. This optimal condition demonstrated a compressive strength of approximately 3.8 N/mm². Kurama et al. [19] also study the use of coal bottom ash from Tuncbilek Thermal Power Plant as an aggregate, increasing its compressive strength gain to 2.78 N/mm². Based on CEB Manual for AAC, standard values of compressive strength, static modulus elasticity, and thermal conductivity for different densities are tabulated in Tab. 2.

Table 2: Properties of AAC [24]

Dry density (kg/m ³)	Compressive strength (MPa)	Static modulus of elasticity (kN/mm ²)	Thermal conductivity (W/m°C)
400	1.3–2.8	0.18–1.17	0.07–0.11
500	2.0–4.4	1.24–1.84	0.08–0.13
600	2.8–6.3	1.76–2.64	0.11–0.17
700	3.9–8.5	2.42–3.58	0.13–0.21

6.2 Thermal Performance

AAC has good thermal insulation due to its cell structure. Thermal performance value (k) is in the range of 0.1–0.7 W/(mK) for dry density values between 400–1700 kg/m³, which is about 2 to 20 times less than the conventional concrete where it is in the range of 1.6–2.0 W/(mK) [64,54,74]. Thermal performance is a dry density function where the thermal performance will also decrease if the density value decreases, as shown in Fig. 3 from below. A decrease in density of 100 kg/m³ induces a decrease in the thermal efficiency of at least 0.02–0.04 W/(mK), based on evidence obtained from previous experimental studies. In testing the thermal performance, the pores and distribution counts are also important.

7 Opportunity for Recycled AAC Waste Powder as a Partial Replacement

In terms of its physical and mechanical properties, the removal of AAC materials such as the use of bottom ash, the inclusion of lead-zinc tailings, blast furnace slag, and recycled plastic aggregates may boost the AAC properties based on the previous study carried out [13,33,52,75]. Such different industrial wastes can be used in the preparation of AAC with the aid of autoclaving. During the autoclaved process, the phase transformation process of C-S-H to form the tobermorite was done under a condition of high pressure and temperature treatment. This tobermorite phase is more stable than the former phase. The micropores were distributed evenly under a high pressure autoclaving. In addition, the existence of the tobermorite phase in AAC plays an important role in providing various outstanding properties [34]. It is undoubtedly important to pay attention to the differences in microstructure and properties, but the

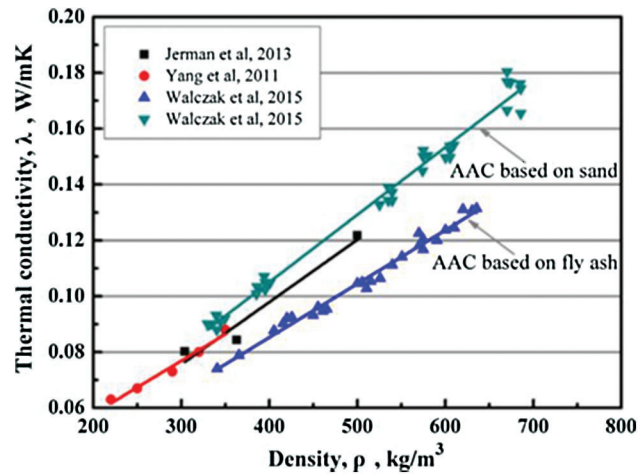


Figure 3: The thermal performance measured by library research as a function of density [64,54,74]

abundance of AAC waste should not be overlooked [11]. Based on previous literature, less of an attempt to use recycled AAC as a partial replacement was reported, particularly building wall concrete. It is found that the aerated concrete demolition waste was used only as fine aggregate in floor screed and to replace cement in building construction [76,77]. Since there is an abundance of AAC waste available, especially in Malaysia, and it is free [11], using recycled AAC in producing a new AAC and improving its properties is an opportunity to be explored. In addition, the use of recycled AAC is a more sustainable approach and reduces the production cost, but it could contribute to the environmental impact.

8 Summary

Summarizing the research about innovations of replacement in AAC materials, the observations from the previous and current studies show that most waste materials used could improve AAC's properties in terms of its physical and mechanical properties. With autoclaving, various industrial wastes can be used to prepare AAC, providing prospective access of industrial by-products and broadening AAC application.

Acknowledgement: The authors acknowledge Solar Energy Research Institute of Universiti Kebangsaan Malaysia for the facilities provided and Nareusan University, Thailand, for the research collaboration.

Funding Statement: The financial supports are from the Ministry of Education Malaysia under the Fundamental Research Grant Scheme (FRGS/1/2018/TK06/UKM/02/1).

Conflicts of Interest: The authors declare that they have no conflicts of interest to report regarding the present study.

References

1. Liu, R., Huang, Y. (2018). Heat and moisture transfer characteristics of multilayer walls. *Energy Procedia*, 152, 324–329. DOI 10.1016/j.egypro.2018.09.142.
2. Stumm, A., Schweike, U., Stemmermann, P. (2018). Nanostructured high insulating autoclaved aerated concrete. *Mauerwerk*, 22(5), 329–334. DOI 10.1002/dama.201800024.
3. Lee, S. W., Lim, C. H., Chan, S. A., Von, K. L. (2017). Techno-economic evaluation of roof thermal insulation for a hypermarket in equatorial climate: Malaysia. *Sustainable Cities and Society*, 35, 209–223. DOI 10.1016/j.scs.2017.08.011.
4. Hussin, A., Haw, L. C., Salleh, E. (2019). Air conditioning energy profile and intensity index for retrofitted Mosque building: A case study in Malaysia. *Alam Cipta*, 12(1), 17–27.

5. Haw, L. C., Aun, C. S. (2019). The impact of air gaps on the performance of reflective insulations. *Alam Cipta*, 12(1), 28–34.
6. Jahandideh, F., Raman, S. N., Jamil, M., Syed, Z. I. (2020). Carbon footprint assessment in the life-cycle design of concrete structures in the tropics: A case study of residential buildings in Malaysia. *Journal of Design and Built Environment*, 20, 27–34.
7. Kubissa, W., Jaskulski, R., Reiterman, P. (2017). Ecological concrete based on blast-furnace cement with incorporated coarse recycled concrete aggregate and fly ash addition. *Journal of Renewable Materials*, 5(1), 53–61. DOI 10.7569/JRM.2017.634103.
8. Cabrillac, R., Fiorio, B., Beaucour, A. L., Dumontet, H., Ortolà, S. (2006). Experimental study of the mechanical anisotropy of aerated concretes and of the adjustment parameters of the introduced porosity. *Construction and Building Materials*, 20(5), 286–295. DOI 10.1016/j.conbuildmat.2005.01.023.
9. Koronthalyova, O. (2011). Moisture storage capacity and microstructure of ceramic brick and autoclaved aerated concrete. *Construction and Building Materials*, 25(2), 879–885. DOI 10.1016/j.conbuildmat.2010.06.098.
10. Hussin, M. W., Muthusamy, K., Zakaria, F. (2010). Effect of mixing constituent toward engineering properties of POFA cement-based aerated concrete. *Journal of Materials in Civil Engineering*, 22(4), 287–295. DOI 10.1061/(ASCE)0899-1561(2010)22:4(287).
11. Rafiza, A. R., Chan, H. Y., Thongtha, A., Jettipattaranat, W., Lim, K. L. (2019). An innovative autoclaved aerated concrete (AAC) with recycled AAC powder for low carbon construction. *IOP Conference Series: Earth and Environmental Science*, 268(1), 012050. DOI 10.1088/1755-1315/268/1/012050.
12. Khedari, J., Watsanasathaporn, P., Hirunlabh, J. (2005). Development of fibre-based soil-cement block with low thermal conductivity. *Cement and Concrete Composites*, 27(1), 111–116. DOI 10.1016/j.cemconcomp.2004.02.042.
13. Agopyan, V., Savastano, H., John, V. M., Cincotto, M. A. (2005). Developments on vegetable fibre-cement based materials in São Paulo, Brazil: An overview. *Cement and Concrete Composites*, 27(5), 527–536. DOI 10.1016/j.cemconcomp.2004.09.004.
14. Fernández-Jiménez, A., Palomo, A., Criado, M. (2005). Microstructure development of alkali-activated fly ash cement: A descriptive model. *Cement and Concrete Research*, 35(6), 1204–1209. DOI 10.1016/j.cemconres.2004.08.021.
15. Grutzeck, M., Kwan, S., DiCola, M. (2004). Zeolite formation in alkali-activated cementitious systems. *Cement and Concrete Research*, 34(6), 949–955. DOI 10.1016/j.cemconres.2003.11.003.
16. Hwang, E. H., Ko, Y. S., Jeon, J. K. (2007). Effect of polymer cement modifiers on mechanical and physical properties of polymer-modified mortar using recycled waste concrete fine aggregate. *Journal of Industrial and Engineering Chemistry*, 13(3), 387–394.
17. Hwang, E. H., Hwang, T. S. (2007). Comparison of physical properties of PAE polymer-modified mortars from recycled waste artificial marble and waste concrete fine aggregates. *Journal of Industrial and Engineering Chemistry*, 13(4), 585–591.
18. Esmaily, H., Nuranian, H. (2012). Non-autoclaved high strength cellular concrete from alkali activated slag. *Construction and Building Materials*, 26(1), 200–206. DOI 10.1016/j.conbuildmat.2011.06.010.
19. Kurama, H., Topçu, I. B., Karakurt, C. (2009). Properties of the autoclaved aerated concrete produced from coal bottom ash. *Journal of Materials Processing Technology*, 209(2), 767–773. DOI 10.1016/j.jmatprotec.2008.02.044.
20. Mostafa, N. Y. (2005). Influence of air-cooled slag on physicochemical properties of autoclaved aerated concrete. *Cement and Concrete Research*, 35(7), 1349–1357. DOI 10.1016/j.cemconres.2004.10.011.
21. Wang, Q., Chen, Y., Li, F., Sun, T., Xu, B. (2006). Microstructure and properties of silty siliceous crushed stone-lime aerated concrete. *Journal Wuhan University of Technology, Materials Science Edition*, 21(2), 17–20. DOI 10.1007/BF02840830.
22. Bayat, A., Liaghat, G., Sabouri, H., Ashkezari, G. D., Pedram, E. et al. (2019). Experimental investigation on the quasi-static mechanical behavior of autoclaved aerated concrete insulated sandwich panels. *Journal of Sandwich Structures and Materials*. (In Press). DOI 10.1177/1099636219857633.

23. Huang, X. Y., Ni, W., Cui, W. H., Wang, Z. J., Zhu, L. P. (2012). Preparation of autoclaved aerated concrete using copper tailings and blast furnace slag. *Construction and Building Materials*, 27(1), 1–5. DOI 10.1016/j.conbuildmat.2011.08.034.
24. Narayanan, N., Ramamurthy, K. (2000). Structure and properties of aerated concrete: A review. *Cement and Concrete Composites*, 22(5), 321–329. DOI 10.1016/S0958-9465(00)00016-0.
25. Thongtha, A., Maneewan, S., Punlek, C., Ungkoon, Y. (2014). Investigation of the compressive strength, time lags and decrement factors of AAC-lightweight concrete containing sugar sediment waste. *Energy and Buildings*, 84, 516–525. DOI 10.1016/j.enbuild.2014.08.026.
26. Karakurt, C., Kurama, H., Topçu, I. B. (2010). Utilization of natural zeolite in aerated concrete production. *Cement and Concrete Composites*, 32(1), 1–8. DOI 10.1016/j.cemconcomp.2009.10.002.
27. Kalpana, M., Mohith, S. (2020). Study on autoclaved aerated concrete: Review. *Materials Today: Proceedings*, 22, 894–896. DOI 10.1016/j.matpr.2019.11.099.
28. Kunchariyakun, K., Asavapisit, S., Sombatsompop, K. (2015). Properties of autoclaved aerated concrete incorporating rice husk ash as partial replacement for fine aggregate. *Cement and Concrete Composites*, 55, 11–16. DOI 10.1016/j.cemconcomp.2014.07.021.
29. Qu, X., Zhao, X. (2017). Previous and present investigations on the components, microstructure and main properties of autoclaved aerated concrete—A review. *Construction and Building Materials*, 135, 505–516. DOI 10.1016/j.conbuildmat.2016.12.208.
30. Kikuma, J. (2009). Formation of autoclaved aerated concrete studied by in situ X-ray diffraction under hydrothermal condition. *Spring-8 Research Frontiers*, (1), 142–143.
31. Galvánková, L., Másilko, J., Solný, T., Štěpánková, E. (2016). Tobermorite synthesis under hydrothermal conditions. *Procedia Engineering*, 151, 100–107. DOI 10.1016/j.proeng.2016.07.394.
32. Papatzani, S., Paine, K., Calabria-Holley, J. (2015). A comprehensive review of the models on the nanostructure of calcium silicate hydrates. *Construction and Building Materials*, 74, 219–234. DOI 10.1016/j.conbuildmat.2014.10.029.
33. Wongkeo, W., Chaipanich, A. (2010). Compressive strength, microstructure and thermal analysis of autoclaved and air cured structural lightweight concrete made with coal bottom ash and silica fume. *Materials Science and Engineering A*, 527(16–17), 3676–3684. DOI 10.1016/j.msea.2010.01.089.
34. Ungkoon, Y., Sittipunt, C., Namprakai, P., Jetipattaranat, W., Kim, K. et al. (2007). Analysis of microstructure and properties of autoclaved aerated concrete wall construction materials. *Journal of Industrial and Engineering Chemistry*, 13(7), 1103–1108.
35. Güçlüer, K., Ünal, O., Demir, İ., Başpınar, M. S. (2015). An investigation of steam curing pressure effect on Pozzolan additive autoclaved aerated concrete. *Technology Education Management Informatic Journal*, 4(1), 78–82.
36. Mostafa, N. Y., El-Hemaly, S. A. S., Al-Wakeel, E. I., El-Korashy, S. A., Brown, P. W. (2001). Activity of silica fume and dealuminated kaolin at different temperatures. *Cement and Concrete Research*, 31(6), 905–911. DOI 10.1016/S0008-8846(01)00489-6.
37. Mitsuda, T., Sasaki, K., Ishida, H. (1992). Phase evolution during autoclaving process of aerated concrete. *Journal of the American Ceramic Society*, 75(7), 1858–1863. DOI 10.1111/j.1151-2916.1992.tb07208.x.
38. Schreiner, J., Goetz-Neunhoeffler, F., Neubauer, J., Volkmann, S., Bergold, S. et al. (2019). Advanced Rietveld refinement and SEM analysis of tobermorite in chemically diverse autoclaved aerated concrete. *Powder Diffraction*, 34(2), 143–150. DOI 10.1017/S0885715619000149.
39. Bergold, S. T., Goetz-Neunhoeffler, F., Neubauer, J. (2013). Quantitative analysis of C-S-H in hydrating alite pastes by *in-situ* XRD. *Cement and Concrete Research*, 53, 119–126. DOI 10.1016/j.cemconres.2013.06.001.
40. Yang, J., Shi, Y., Yang, X., Liang, M., Li, Y. et al. (2013). Durability of autoclaved construction materials of sewage sludge-cement-fly ash-furnace slag. *Construction and Building Materials*, 48, 398–405. DOI 10.1016/j.conbuildmat.2013.07.018.
41. Albayrak, M., Yörükoğlu, A., Karahan, S., Atlihan, S., Yılmaz Aruntaş, H. et al. (2007). Influence of zeolite additive on properties of autoclaved aerated concrete. *Building and Environment*, 42(9), 3161–3165. DOI 10.1016/j.buildenv.2006.08.003.

42. Cai, L., Ma, B., Li, X., Lv, Y., Liu, Z. et al. (2016). Mechanical and hydration characteristics of autoclaved aerated concrete (AAC) containing iron-tailings: Effect of content and fineness. *Construction and Building Materials*, 128, 361–372. DOI 10.1016/j.conbuildmat.2016.10.031.
43. Hong, S. Y., Glasser, F. P. (2004). Phase relations in the CaO-SiO₂-H₂O system to 200°C at saturated steam pressure. *Cement and Concrete Research*, 34(9), 1529–1534. DOI 10.1016/j.cemconres.2003.08.009.
44. Song, Y., Li, B., Yang, E. H., Liu, Y., Ding, T. (2015). Feasibility study on utilization of municipal solid waste incineration bottom ash as aerating agent for the production of autoclaved aerated concrete. *Cement and Concrete Composites*, 56, 51–58. DOI 10.1016/j.cemconcomp.2014.11.006.
45. Bonakdar, A., Babbitt, F., Mobasher, B. (2013). Physical and mechanical characterization of fiber-reinforced aerated concrete (FRAC). *Cement and Concrete Composites*, 38, 82–91. DOI 10.1016/j.cemconcomp.2013.03.006.
46. Li, Z., Chen, L., Fang, Q., Chen, W., Hao, H. et al. (2017). Experimental and numerical study of basalt fiber reinforced polymer strip strengthened autoclaved aerated concrete masonry walls under vented gas explosions. *Engineering Structures*, 152, 901–919. DOI 10.1016/j.engstruct.2017.09.055.
47. Pehlivanli, Z. O., Uzun, I., Yücel, Z. P., Demir, I. (2016). The effect of different fiber reinforcement on the thermal and mechanical properties of autoclaved aerated concrete. *Construction and Building Materials*, 112, 325–330. DOI 10.1016/j.conbuildmat.2016.02.223.
48. Deng, M., Zhang, W., Yang, S. (2020). In-plane seismic behavior of autoclaved aerated concrete block masonry walls retrofitted with high ductile fiber-reinforced concrete. *Engineering Structures*, 219, 110854. DOI 10.1016/j.engstruct.2020.110854.
49. Wang, C. L., Ni, W., Zhang, S. Q., Wang, S., Gai, G. S. et al. (2016). Preparation and properties of autoclaved aerated concrete using coal gangue and iron ore tailings. *Construction and Building Materials*, 104, 109–115. DOI 10.1016/j.conbuildmat.2015.12.041.
50. Mehmannaavaz, T., Ismail, M., Sumadi, S. R., Bhutta, M. A. R., Samadi, M. et al. (2014). Binary effect of fly ash and palm oil fuel ash on heat of hydration aerated concrete. *Scientific World Journal*, 2014, 1–6. DOI 10.1155/2014/461241.
51. Cong, X. Y., Lu, S., Yao, Y., Wang, Z. (2016). Fabrication and characterization of self-ignition coal gangue autoclaved aerated concrete. *Materials and Design*, 97, 155–162. DOI 10.1016/j.matdes.2016.02.068.
52. Ma, B. G., Cai, L. X., Li, X. G., Jian, S. W. (2016). Utilization of iron tailings as substitute in autoclaved aerated concrete: Physico-mechanical and microstructure of hydration products. *Journal of Cleaner Production*, 127, 162–171. DOI 10.1016/j.jclepro.2016.03.172.
53. Różycka, A., Pichór, W. (2016). Effect of perlite waste addition on the properties of autoclaved aerated concrete. *Construction and Building Materials*, 120, 65–71. DOI 10.1016/j.conbuildmat.2016.05.019.
54. Walczak, P., Małolepszy, J., Reben, M., Szymański, P., Rzepa, K. (2015). Utilization of waste glass in autoclaved aerated concrete. *Procedia Engineering*, 122, 302–309. DOI 10.1016/j.proeng.2015.10.040.
55. Serhat Baspinar, M., Demir, I., Kahraman, E., Gorhan, G. (2014). Utilization potential of fly ash together with silica fume in autoclaved aerated concrete production. *KSCE Journal of Civil Engineering*, 18(1), 47–52. DOI 10.1007/s12205-014-0392-7.
56. Wongkeo, W., Thongsanitgarn, P., Pimraksa, K., Chaipanich, A. (2012). Compressive strength, flexural strength and thermal conductivity of autoclaved concrete block made using bottom ash as cement replacement materials. *Materials and Design*, 35, 434–439. DOI 10.1016/j.matdes.2011.08.046.
57. Ungkoon, Y., Sittipunt, C., Namprakai, P., Jetipattaranat, W., Kim, K. S. et al. (2007). Analysis of microstructure and properties of autoclaved aerated concrete wall construction materials. *Journal of Industrial and Engineering Chemistry*, 13(7), 1103–1108.
58. Rosti, A., Penna, A., Rota, M., Magenes, G. (2016). In-plane cyclic response of low-density AAC URM walls. *Materials and Structures*, 49(11), 4785–4798. DOI 10.1617/s11527-016-0825-5.
59. Bate, S. C. C. (1979). Guide for structural lightweight aggregate concrete: Report of ACI committee 213. *International Journal of Cement Composites and Lightweight Concrete*, 1(1), 5–6. DOI 10.1016/0262-5075(79)90004-6.

60. Chaipanich, A., Chindaprasirt, P. (2015). *The properties and durability of autoclaved aerated concrete masonry blocks. Eco-efficient masonry bricks and blocks: Design, properties and durability*, UK: Elsevier Ltd. DOI 10.1016/B978-1-78242-305-8.00009-7
61. Ramamurthy, K., Kunhanandan Nambiar, E. K., Indu Siva Ranjani, G. (2009). A classification of studies on properties of foam concrete. *Cement and Concrete Composites*, 31(6), 388–396. DOI 10.1016/j.cemconcomp.2009.04.006.
62. Kavita, M., Tarjani, C. (2016). Comparison on auto aerated concrete to normal concrete. *Global Research and Development Journal for Engineering*, 1(Special Issue RCEGS 2016), 90–94.
63. Lam, N. T., Asamoto, S., Matsui, K. (2018). Microstructure and shrinkage behavior of autoclaved aerated concrete (AAC)—Comparison of Vietnamese and Japanese AACs. *Journal of Advanced Concrete Technology*, 16(8), 333–342. DOI 10.3151/jact.16.333.
64. Jerman, M., Keppert, M., Výborný, J., Černý, R. (2013). Hygric, thermal and durability properties of autoclaved aerated concrete. *Construction and Building Materials*, 41, 352–359. DOI 10.1016/j.conbuildmat.2012.12.036.
65. Goual, M. S., Bali, A., de Barquin, F., Dheilly, R. M., Quéneudec, M. (2006). Isothermal moisture properties of Clayey Cellular Concretes elaborated from clayey waste, cement and aluminium powder. *Cement and Concrete Research*, 36(9), 1768–1776. DOI 10.1016/j.cemconres.2005.12.017.
66. Zhang, P., Wittmann, F. H., Vogel, M., Müller, H. S., Zhao, T. (2017). Influence of freeze-thaw cycles on capillary absorption and chloride penetration into concrete. *Cement and Concrete Research*, 100, 60–67. DOI 10.1016/j.cemconres.2017.05.018.
67. Yi, S. Y., Fan, L. W., Fu, J. H., Xu, X., Yu, Z. T. (2016). Experimental determination of the water vapor diffusion coefficient of autoclaved aerated concrete (AAC) via a transient method: Effects of the porosity and temperature. *International Journal of Heat and Mass Transfer*, 103, 607–610. DOI 10.1016/j.ijheatmasstransfer.2016.07.111.
68. Wu, H., Liu, C., Shi, S., Chen, K. (2020). Experimental research on the physical and mechanical properties of concrete with recycled plastic aggregates. *Journal of Renewable Materials*, 8(7), 727–738. DOI 10.32604/jrm.2020.09589.
69. Kočí, V., Maděra, J., Jerman, M., Černý, R. (2018). Experimental determination of frost resistance of autoclaved aerated concrete at different levels of moisture saturation. *International Journal of Thermophysics*, 39(6), 1–11. DOI 10.1007/s10765-017-2325-4.
70. Hoff, G. C. (1972). Porosity-strength considerations for cellular concrete. *Cement and Concrete Research*, 2(1), 91–100. DOI 10.1016/0008-8846(72)90026-9.
71. Kikuma, J., Tsunashima, M., Ishikawa, T., Matsuno, S., Ogawa, A. et al. (2011). *In situ* time-resolved X-ray diffraction of tobermorite synthesis process under hydrothermal condition. *IOP Conference Series: Materials Science and Engineering*, 18, 022017. DOI 10.1088/1757-899X/18/2/022017.
72. Jitchaiyaphum, K., Sinsiri, T., Jaturapitakkul, C., Chindaprasirt, P. (2013). Cellular lightweight concrete containing high-calcium fly ash and natural zeolite. *International Journal of Minerals, Metallurgy and Materials*, 20(5), 462–471. DOI 10.1007/s12613-013-0752-1.
73. Wang, C., Liu, Z., Li, J., Jiao, S., Zhang, Y. (2017). Study on preparation of autoclaved aerated concrete using lead-zinc tailings. *Chemical Engineering Transactions*, 62, 931–936. DOI 10.3303/CET1762156.
74. Bulletins, C. E. B., (1977). CEB Manual of Autoclaved Aerated Concrete Design and Technology (PDF). (n.d.). 2020. <https://www.fib-international.org/publications/ceb-bulletins/ceb-manual-of-autoclaved-aerated-concrete-design-and-technology-detail.html>.
75. Yang, R., Zhu, J., Wu, Z., Wu, Z., Li, M. et al. (2011). Thermal insulation and strength of autoclaved light concrete. *Journal of Wuhan University of Technology, Materials Science Edition*, 26(1), 132–136. DOI 10.1007/s11595-011-0184-6.
76. Bergmans, J., Nielsen, P., Snellings, R., Broos, K. (2016). Recycling of autoclaved aerated concrete in floor screeds: Sulfate leaching reduction by ettringite formation. *Construction and Building Materials*, 111, 9–14. DOI 10.1016/j.conbuildmat.2016.02.075.
77. He, X., Zheng, Z., Yang, J., Su, Y., Wang, T. et al. (2020). Feasibility of incorporating autoclaved aerated concrete waste for cement replacement in sustainable building materials. *Journal of Cleaner Production*, 250, Article no.: 119455. DOI 10.1016/j.jclepro.2019.119455.